

ACOUSTICAL LETTER

Sound insulation characteristics of small fixed windows in a laboratory and prediction with an existing theory

Marie Mimura[1,3,*], Yohei Tsukamoto[2,3], Yoshihiro Tomikawa[2], Takeshi Okuzono[3] and Kimihiro Sakagami[3]

[1]*Technology and Innovation Center, YKK Corporation, 200 Yoshida, Kurobe, 938–8601 Japan*
[2]*Central Research Laboratory, YKK AP Inc., YKK AP R&D Center, 1 Ogyu, Kurobe, 938–8612 Japan*
[3]*Environmental Acoustic Laboratory, Department of Architecture, Graduate School of Engineering, Kobe University, 1–1 Rokkodai-cho, Nada-ku, Kobe, 657–8501 Japan*

(*Received 4 March 2022, Accepted for publication 11 April 2022*)

Keywords: Reverberation room, Sound insulation, Sound transmission loss, Window

1. Introduction

Accurate prediction of the sound insulation performance of windows is an important topic because a window is an essential building component affecting the indoor sound environment of dwellings. Although some theories [1,2] have been used to predict the sound reduction index *SRI* of single plates, wave-based vibroacoustic numerical analysis [3] can be used for accurate assessment of airborne and structure-borne sound propagation for windows of various types with a complex frame structure under appropriate numerical modeling. Nevertheless, even for fixed windows, which are the simplest window type, having a single glass and a simple frame structure, the predictive accuracy of numerical analyses has not been examined in detail because insufficient measured data are available for use as a reference for numerical analysis. Because window sizes are well known to affect *SRI*, verifying the predictive accuracy of numerical analyses for windows of various sizes used in actual dwellings is important. Although earlier studies [4–6] have indicated that the *SRI* of single plate decreases as size increases at a coincidence frequency f_c, different tendencies have been reported below f_c. Earlier studies on window size effect [7,8] also have indicated that *SRI* have small differences in size below f_c, but have not studied above f_c. However, we still need to clarify how the window size affects the sound insulation performance of fixed windows in detail with the discussions on the vibration characteristics and the energy loss factor of the vibrations in the window since they are highly associated with their sound insulation characteristics. These discussions on the fixed windows are not available in earlier works and will be helpful for understanding and modeling of sound insulation performance of fixed windows.

This study presents a discussion on the sound insulation characteristics of fixed windows in a laboratory, specifically focusing on the window size effect. Our study includes showing the vibration characteristic and the total loss factors of fixed windows, to elucidate details of effects related to window size. Additionally, we examined whether or not an existing theory explains measured *SRI*s of various-sized fixed windows, with a measured loss factor.

*e-mail: m-mimura@ykk.com
[doi:10.1250/ast.43.276]

2. Measurements

2.1. Experiment outline and settings

We measured *SRI*s of five fixed windows with area of $0.2\,m^2$ to $2.0\,m^2$ in irregularly shaped reverberant rooms according to JIS A 1416 [9]. The source reverberant room has $492.8\,m^3$ volume. The receiving reverberant room has $264.5\,m^3$ volume. Figure 1 portrays a fixed window of $W \times H$ size mounted on a test opening. Table 1 presents detailed dimensions of the five windows (A)–(E). Windows (A)–(D) have a similar aspect ratio of around 1.6, which is determined by the golden ratio. Window (E) has the same area as that of window (C), but it has a different aspect ratio of 3.27. Each window comprises a float glass pane with 5 mm thickness and a frame made of aluminum and PVC. The windows were mounted on a wooden frame filled with mortar with 18–36 screws. Gypsum board was mounted on the wooden frame. Then we placed them in a $2\,m \times 2\,m$ opening in the reverberation chambers. The gap between the wooden frame and the opening was sealed with clay. In addition, the gap between the wooden frame and the window frame was sealed with tape to minimize the sound leakage. The wooden frames have sufficiently high surface density of $450\,kg/m^2$, which is heavier than the surface density $12.5\,kg/m^2$ of glass. However, windows smaller than $1\,m^2$ present the concern that the wooden frame's sound insulation performance might adversely affect the window's sound insulation performance because the wooden frame occupies a large fraction of the area of the opening. Therefore, for the two small windows (A) and (B), we mounted six and two windows to the wooden frames, as shown in Fig. 2. Their *SRI*s were calculated by dividing the sample numbers.

We also measured vibration velocity distributions on the glass surface using accelerometers (352A92, 352A59; PCB Piezotronics Inc. and NP-3211; Ono Sokki Co., Ltd.) under the same sound source condition as in the sound insulation test. The accelerometers were mounted on glass at equal intervals of at least 18 points in a horizontal direction and at least 6 points in a vertical direction. The wax (NP-0010; Ono Sokki Co., Ltd.) was used to mount the accelerometers on the

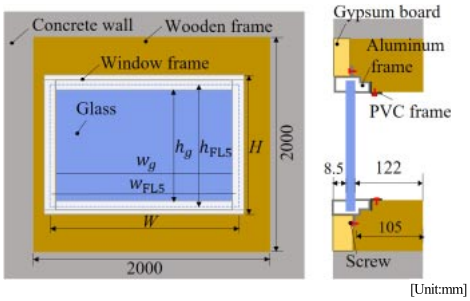

Fig. 1 Appearance of tested windows mounted on a test opening in reverberation chambers. Front view in (left) and side view in (right). A cross-section of the window frame is depicted in simplified form.

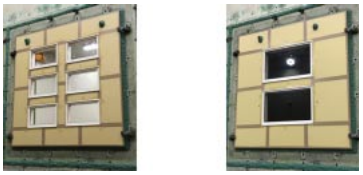

Fig. 2 Mounting condition of (left) Window (A) and (right) Window (B).

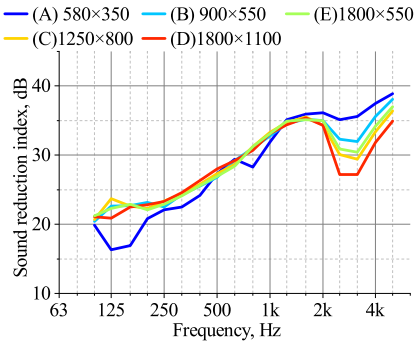

Fig. 3 *SRI* for five fixed windows (A)–(E).

glass where a small amount of wax was applied between the glass and the accelerometers, and then the accelerometers were pressed with a finger to fix it on the window's surface. An accelerometer, which was used for the reference of phase, was placed at a point on the wooden frame far from the window.

The total loss factor η_{tot} of each window was calculated from structural reverberation time T_{s} obtained using a impulse test with a steel ball pendulum [4]. The structural reverberation times were estimated using an integrated impulse response method from vibration signals via one-third octave band filters. With the T_{s}, the total loss factor η_{tot} was calculated at one-third octave band center frequencies f_{m} as

$$\eta_{\mathrm{tot}} = \frac{2.2}{f_{\mathrm{m}} T_{\mathrm{s}}}. \qquad (1)$$

We took total loss factor measurements five times with three excitation points and three measured positions; then their averaged value was computed. The same mounting condition as those used for the vibration test was used for accelerometers. The upper-limit of measurable η_{tot} is 0.22 because of the filter transient.

2.2. Results and discussion

Figure 3 presents a comparison of *SRI*s among five fixed windows (A)–(E). It shows that, although slight variation in *SRI*s is apparent around 125 Hz, no size dependence is apparent at frequencies below a coincidence frequency f_{c}, except for the smallest window (A), where the *SRI*s show almost identical levels for four windows (B)–(E) with area of 0.5–2.0 m^2. The maximum difference of *SRI*s between windows (B)–(E) is 1.2 dB at frequencies above 125 Hz and below f_{c}. The results of several cases of difference in size are similar to those reported from earlier studies of windows [7,8], but our results show less size-dependence. Clear size dependence is apparent at frequencies higher than f_{c}, indicating that larger windows have smaller *SRI* values. This result agrees with those obtained from earlier studies conducted for a single plate [4–6]. The smallest window (A) has a large dip at 125 Hz and slight dips at 315 Hz and 800 Hz, which are not apparent for other windows.

Figure 4 presents a comparison of measured normal mode shapes for windows (A)–(E), with mode numbers (m,n). We were able to identify the mode shapes up to 570 Hz for window (A) and 200–250 Hz for the other windows but we were unable to identify higher frequencies above those frequencies because of high modal density. Results show that a first normal mode (1, 1), at which all parts of glass move in phase, exists at 125 Hz. It is the cause of the deep dip for the *SRI* of window (A). In addition, window (A) has the lowest modal density. It can contribute to variance in *SRI* at frequencies lower than 1 kHz. Other windows (B)–(E) have no (1, 1) mode within the measured frequency range. Higher modes can show a small contribution to sound radiation because of lower radiation efficiencies.

Figure 5 portrays the average surface velocity level L_{v}, which is an energetic average level calculated over measured points. The figure shows that L_{v} has clear size dependence at

Table 1 Dimensions of five fixed windows.

Window	Window size $W \times H$, mm	Glass size $w_{\mathrm{FL5}} \times h_{\mathrm{FL5}}$, mm	Exposed glass size $w_{\mathrm{g}} \times h_{\mathrm{g}}$, mm	Area, m^2	Aspect ratio
(A)	580 × 350	523 × 299	508 × 284	0.2	1.66
(B)	900 × 550	843 × 499	828 × 484	0.5	1.64
(C)	1,250 × 800	1,193 × 749	1,178 × 734	1.0	1.56
(D)	1,800 × 1,100	1,743 × 1,049	1,728 × 1,034	2.0	1.64
(E)	1,800 × 550	1,743 × 499	1,728 × 484	1.0	3.27

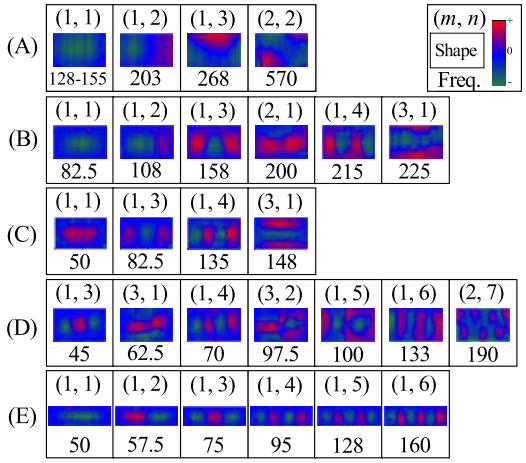

Fig. 4 Normal mode shapes of the five fixed windows (A)–(E).

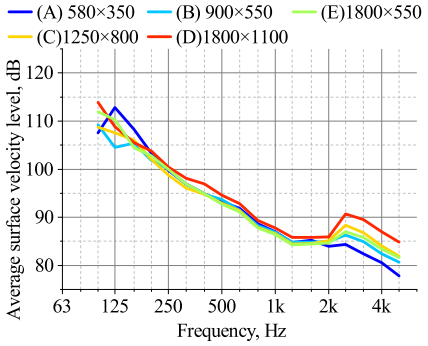

Fig. 5 Average surface velocity levels for five fixed windows (A)–(E).

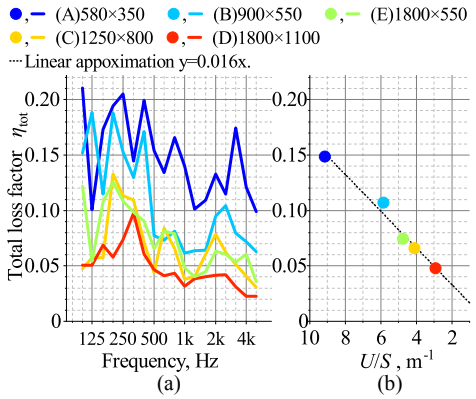

Fig. 6 Total loss factors η_{tot} of five fixed windows (A)–(E): (a) frequency characteristics and (b) relations between the averaged η_{tot} for all frequencies and the parameter $\frac{U}{S}$.

frequencies higher than f_c; larger windows show higher L_v. In addition, window (A) shows the highest L_v at 125 Hz.

Figures 6(a) and 6(b) respectively portray frequency characteristics of the η_{tot} of the five windows and the relation between the averaged η_{tot} for all frequencies and parameter $\frac{U}{S}$, where U and S respectively represent the window perimeter and area. Note that η_{tot} is expressed as the sum of three loss factors, namely the internal loss factor, the boundary loss factor, and the radiation loss factor. Because premeasurement of the internal loss factor of the glass is a pretty small value of 0.002, including the radiation loss factor, we assumed the boundary loss factor has a dominant role in the η_{tot}. With this assumption, we guessed that the η_{tot} is associated with the parameter $\frac{U}{S}$, which is appeared in the expression of the boundary loss factor by Craik [10], and then the averaged η_{tot} was evaluated as a function of $\frac{U}{S}$. Results show that the η_{tot} increases as the window size decreases. The η_{tot}s in window (A) show a small value at 125 Hz and a large value at f_c. They correspond to *SRI* dips at 125 Hz and the large *SRI* value at f_c. In addition, the η_{tot} has strong correlation to the parameter $\frac{U}{S}$. It decreases linearly with decreasing $\frac{U}{S}$ and this relation will be useful when estimating η_{tot} of other size of fixed windows.

3. Prediction by existing theory using measured total loss factor

3.1. Theory

In general, the *SRI* of a single construction at the random incidence is calculated as the sum of the sound reduction index of the forced transmission SRI_f and resonant transmission SRI_r, as [2]

$$SRI = -10\log_{10}(10^{-0.1SRI_f} + 10^{-0.1SRI_r}), \tag{2}$$

where SRI_f is expressed by the wall impedance model based on the bending wave equation. It includes the contribution of the first normal mode of a single plate. The finite plate size effect is modeled using the radiation efficiency σ_f. For σ_f, Sewell's equation [1] is used at the range of $ka > 0.5$, where k is the wavenumber in air and where a is the characteristic dimension of a plate. For $ka < 0.5$, it is defined as $\sigma_f = \frac{2(ka)^2}{\pi}$ [11]. The SRI_f is expressed as

$$SRI_f = SRI_0 + 10\log_{10}\left\{\left(1 - \left(\frac{f_{11}}{f}\right)^2\right)^2 \cdot \left(1 - \left(\left(\frac{c}{c_s}\right)^2 + \left(\frac{f_c}{f}\right)^2\right)^{-1}\right)^2 + \eta_{tot}^2\right\} - 10\log_{10}\sigma_f, \tag{3}$$

where SRI_0 stands for the mass law, f represents the frequency, f_{11} denotes the first natural frequency of a plate with a simply supported boundary, c expresses the speed of sound, and c_s denotes the speed of the shear wave of a plate. The resonant transmission SRI_r is described, based on the statistical energy analysis as

$$SRI_r = SRI_0 - 10\log_{10}\left(\frac{c^2\sigma_r^2}{2\eta_{tot}Sf} \cdot \frac{\Delta N}{\Delta f}\right), \tag{4}$$

where $\frac{\Delta N}{\Delta f}$ stands for the modal density of the bending wave of a plate, and σ_r represents the radiation efficiency of the resonant vibration at random incidence defined as shown below [11].

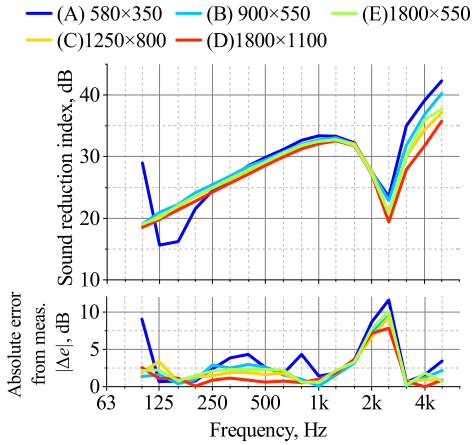

Fig. 7 Theoretically predicted *SRI*s of five fixed windows (A)–(E) and the absolute error $|\Delta e|$ between theory and measurement.

$$\sigma_{\mathrm{r}} = \begin{cases} \dfrac{c^2}{Sf_{\mathrm{c}}^2} g_1(M) + \dfrac{Uc}{Sf_{\mathrm{c}}} g_2(M) & (f_{11} < f < f_{\mathrm{c}}) \\ \sqrt{\dfrac{\pi f U}{16c}} & (f \simeq f_{\mathrm{c}}) \\ (1 - M^{-2})^{-\frac{1}{2}} & (f > f_{\mathrm{c}}) \end{cases} . \quad (5)$$

Therein, M $(= \sqrt{\frac{f}{f_{\mathrm{c}}}})$ is the Mach number, and g_1 and g_2 are help functions. The use of the first equation in Eq. (5) for a small window is a trial because it is derived with the assumption of high modal density.

For this study, we used measured η_{tot} in Fig. 6(a) for the theory presented above. In addition, the material properties of glass were assumed as Young's modulus of 7.16×10^{10} Pa, density of 2,500 kg/m^3, Poisson's ratio of 0.23, and 5 mm thickness.

3.2. Results and discussion

Figure 7 shows the theoretical *SRI*s of five fixed windows (A)–(E) and the absolute errors of *SRI*s between measurements and theoretically calculated results. The theoretical results reproduce the measured trend qualitatively, as shown in Fig. 3. In the theoretical results, the size dependence on *SRI* cannot be found at frequencies below f_{c}, except for the smallest window (A). The dip by the first mode in the smallest windows (A) at 125 Hz is also reproduced. Furthermore, the *SRI* decreases as the size increases above f_{c}, which is consistent with the measurement. However, quantitatively, larger discrepancies can be found for smaller windows and especially for around at f_{c} in all windows. At frequencies 250 Hz–1 kHz, the absolute error from the measurement is 4.3 dB at 400 Hz in the smallest window (A) and 1.6 dB in the largest window (D). On the other hand, the error value around f_{c} reaches 8–12 dB despite using the measured total loss factor.

Possible reasons for the large discrepancy are that the theory does not consider the window frame structure and the laboratory environment. Additionally, a difference in the boundary conditions might exist between measured and theoretically calculated results. Future studies will be conducted to clarify how numerical analysis can improve the predictive accuracy.

4. Conclusion

We revealed windows size effect on the sound insulation characteristics of five fixed windows of 0.2–2.0 m^2 in a laboratory, discussing the relation between *SRI* and their vibration characteristics and η_{tot}s. We also examined whether or not an existing theory can explain the measured results when using the measured η_{tot}. The results are summarized below.

(1) Apparent window size effects on *SRI* are not observed for fixed windows of 0.2–2.0 m^2, except for the smallest windows at frequencies below f_{c}. In addition, larger fixed windows have lower *SRI* above f_{c}.

(2) The *SRI* of a small fixed window shows a dip at the first normal mode f_{11} if f_{11} is included within the measured frequency range.

(3) The η_{tot} of fixed windows becomes large for smaller windows. Its frequency-averaged value shows strong correlation with the parameter $\frac{U}{S}$. The averaged value decreases linearly as $\frac{U}{S}$ decreases.

(4) Existing theory for a single construction using measured η_{tot}s can explain the tendency of measured *SRI* of fixed windows qualitatively. However, it shows larger discrepancies on *SRI* for smaller windows.

References

[1] E. C. Sewell, "Transmission of reverberant sound through single-leaf partition surrounded by an infinite rigid baffle," *J. Sound Vib.*, **12**, 21–32 (1970).

[2] J. H. Rindel, "Airborne sound transmission through single constructions," in *Sound Insulation in Buildings* (CRC Press, Boca Raton, 2018), Chap. 8, pp. 203–245.

[3] M. Mimura, T. Okuzono and K. Sakagami, "Pilot study on numerical prediction of sound reduction index of double window system: Comparison of finite element prediction method with measurement," *Acoust. Sci. & Tech.*, **43**, 32–42 (2022).

[4] J. Yoshimura, S. Sugie and E. Toyoda, "Effects of size and edge damping on measurement results for sound reduction index of glass pane," *Proc. Inter-Noise 2006*, No. 641, 10 pages (2006).

[5] R. W. Guy, A. Demey and P. Sauer, "The effect of some physical parameters upon the laboratory measurements of sound transmission loss," *Appl. Acoust.*, **18**, 81–98 (1985).

[6] R. R. Wareing, J. L. Davy and J. R. Pearse, "Variations in measured sound transmission loss due to sample size and construction parameters," *Appl. Acoust.*, **89**, 166–177 (2015).

[7] N. Michelsen, "Effect of size on measurements of the sound reduction index of a window or a pane," *Appl. Acoust.*, **16**, 215–234 (1983).

[8] Y. Tsukamoto, K. Sakagami, T. Okuzono and Y. Tomikawa, "Basic considerations on the practical method for predicting sound insulation performance of a single-leaf window," *UCL Open: Environment*, **2**, 06 (2021).

[9] JIS A 1416:2000 Acoustics — Method for laboratory measurement of airborne sound insulation of building elements (2000).

[10] R. J. M. Craik, "Damping of building structures," *Appl. Acoust.*, **14**, 347–359 (1981).

[11] J. H. Rindel, "Sound radiation from plates," in *Sound Insulation in Buildings* (CRC Press, Boca Raton, 2018), Chap. 6, pp. 155–187.